Comparative life cycle assessment of merging recycling method for spent electric vehicle lithium ion batteries

ZhiWen Zhou [a, b], Yiming Lai [a, b], Qin Peng [a, b], Jun Li [* a, b]

[a] Key Laboratory of Low-grade Energy Utilization Technologies and Systems, Chongqing University, Ministry of Education, Chongqing 400044, China;

[b] Institute of Engineering Thermophysics, Chongqing University, Chongqing 400044, China;

[*] Corresponding authors:

Emails: lijun@cqu.edu.cn (Jun Li),

Tel./fax: +86 23 65102474.

Table S1 Energy consumption and GHG emissions associated with different transportation modes.

Modes		Energy Consumption [MJ_{-eq} $(t \cdot km)^{-1}$]	GHG Emissions [kg $CO_{2\text{-}eq}$ $(t \cdot k)^{-1}$]	Resource
Freight transport by road	lorry 3.5-7.5 t	8.24	0.51	Ecoinvent v3.5
	lorry >32 t	1.56	0.09	Ecoinvent v3.5

Table S2 Material inventories for EV LIBs.

Materials [a]	(wt%)
Active Material ($LiCoO_2$)	29
Wrought Aluminum	20
Copper	11
Graphite/Carbon	18
Electrolyte: Ethylene Carbonate	5.4
Electrolyte: Dimethyl Carbonate	5.4
Electrolyte: $LiPF_6$	1.9
Electronic Parts	1.4
Steel	1.4
Binder (polyvinylidene fluoride, PVDF)	2.5
Polypropylene	1.6
Polyethylene	0.28
Polyethylene Terephthalate	1.2
Glycol (coolant)	1.1
Thermal Insulation	0.37
Cells [b]	78.63
Total（kg）	170
Capacity（mAh/g）	150

[a] The battery pack and prismatic pouch cell structure and composition were based on previous studies [1, 2].

[b] The cells consist of the following components: active materials, graphite/carbon, electrolyte: ethylene carbonate, electrolyte: dimethyl carbonate, electrolyte: $LiPF_6$, binder, Polypropylene, polyethylene, polyethylene terephthalate, aluminum (cathode current collector, cell housing) and copper (anode current collector). We assumed that the aluminum in the cells takes a proportion of 20% of the total wrought aluminum used and the copper in cells occupy 85% of the total copper used according to ref. [3-5].

Table S3 Carbon-containing components in lithium-ion battery cells and their carbon contents. [3]

Component	kg C kg^{-1} component
Polyethylene terephthalate（PET）	0.63
Polypropylene（PP）	0.86
Polyethylene（PE）	0.92
Carbon/graphite	1
Ethylene carbonate（EC）	0.41
Dimethyl carbonate（DC）	0.4
PVDF	0.36

Table S4 Energy consumption and GJG emissions associated with chemicals used in LIB recycling.

Materials	Production Energy Consumption (MJ kg^{-1})	Production GHG Emissions (kg $CO_{2\text{-eq}}$ kg^{-1})	Resource
H_2O_2	23.2	1.18	Ecoinvent v3.5
H_2SO_4	0.2	0.01	[6]
Citric acid	38	1.5	[6]
Li_2CO_3	31.83	2.16	Ecoinvent v3.5
Na_2CO_3	4.79	0.31	Ecoinvent v3.5
NaCl	1.97	0.1	Ecoinvent v3.5
CO_2 (liquid)	9.58	0.71	Ecoinvent v3.5
N_2 (liquid)	6.18	0.24	Ecoinvent v3.5
Ar (liquid)	38.77	1.52	Ecoinvent v3.5
Diesel	3.01	0.36	Ecoinvent v3.5
Coke[a]	1.17	0.017	Ecoinvent v3.5
Limestone	0.058	0.0023	Ecoinvent v3.5
Primary copper	48.19	3.55	Ecoinvent v3.5
Secondary copper	29.51	2.32	Ecoinvent v3.5
Primary aluminum	213	17	[7]
Secondary aluminum	10.4	0.72	[7]
$LiCoO_2$	147	13	[8, 9]
Deionised water	0.022	0.0015	Ecoinvent v3.5

[a]: The net calorific value of coke was 28.6 MJ/kg [Ecoinvent v3.5] with a carbon content of 83.34 wt% [10].

Table S5 GHG emissions associated with different electricity structure.

Electricity Grid	GHG Emissions (kg $CO_{2\text{-}eq}$/kWh)	Resource
Guangdong	0.84	
Shandong	1.16	Ecoinvent v3.5
Sichuan	0.28	

Table S6 Sulfuric acid leaching conditions for recycling of valuable metals from LIBs [*]

Refe-rence	H_2SO_4 con-centration	H_2O_2 con-Centration (vol.%)	S/L ratio [b] （g mL^{-1}）	Tempera-ture（℃）	Time （min）	Leaching results
[11]	2 M	15	50	75	10	Li （100%） Co （100%）
[12]	2 M	5	100	75	30	Li （93%） Co （94%）
[13]	6 Vol.%	1	33.33	65	60	Li （95%） Co （80%）
[14]	4 Vol.%	1	33.33	40	60	Li （100%） Co （97%）
[15]	2 M	6	100	60	60	Li （97%） Co （98%）
[16]	2 M	5	50	80	60	Li （99%） Co （99%）
[17]	4 M	10	100	85	120	Li （96%） Co （95%）
[18]	2 M	2	33	60	120	Li （87.5%） Co （96.3%）
[19]	2 M	5	100	75	60	Li （99%） Co （70%）
[20]	2 M	8	50	75	60	Li （-） Co （98%）

[a] The reagent consumption for sulfuric acid leaching were calculated based on the average experimental value reported in Table S6.

Table S7 Citric acid leaching conditions for recycling of valuable metals from LIBs*

Refe-rence	Citric acid concentration	H_2O_2 con-centration	S/L ratio b （g mL^{-1}）	Tempera-ture（℃）	Time （min）	Leaching results
[21]	2 M	0.6 g/g (H_2O_2/LCO)	50	70	80	Li （99%） Co （98%）
[22]	1.25 M	1 vol.%	20	90	30	Li （100%） Co （90%）
[23]	2 M	1.25 vol.%	30	60	120	Li （92.53%） Co （81.5%）
[24]	1 M	8% (V_{H2O2} /V_{Citric})	40	70	70	Li （99%） Co （99%）
[25]	2 M	3 v/v% of H_2O_2 30 v/v%	20	80	90	Li （99%） Co （99%）
[26]	2 M	0.25 M	20	80	120	Li （98%） Co （98%）
[27]	1 M	1 vol.%	20	90	30	Li （99.6%） Co （97.6%）
[28]	0.5 M	0.55 M	25	60	300	Li （100%） Co （96%）

[a] The reagent consumption for citric acid leaching were calculated based on the average experimental value reported in Table S7.

Descriptions of life cycle inventories

1. Collection and transportation phase

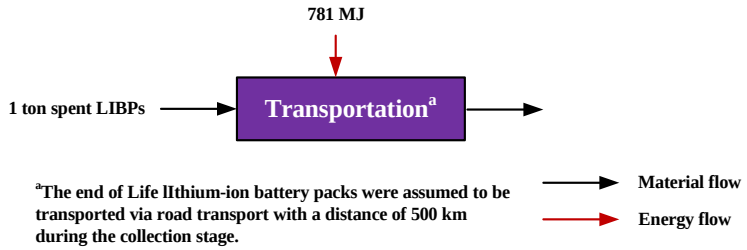

Figure S1. Energy and material flows for the collection and transportation phase of spent LIB recycling system.

In this study, the spent LIBs were transported by road, and the distance from the collection site to the recycling plant was 500 km due to the safety problem resulting from the thermal runaway of LIBs, and the energy consumption of the lorry was 1.56 MJ $(t \cdot km)^{-1}$ (lorry > 32t, Ecoinvent v3.5) [29, 30]. As shown in Fig. S1, when 1 FU of spent LIBPs was inputted in the system, the total energy consumption for the collection and transportation phase was 781 MJ.

2. Pretreatment phase

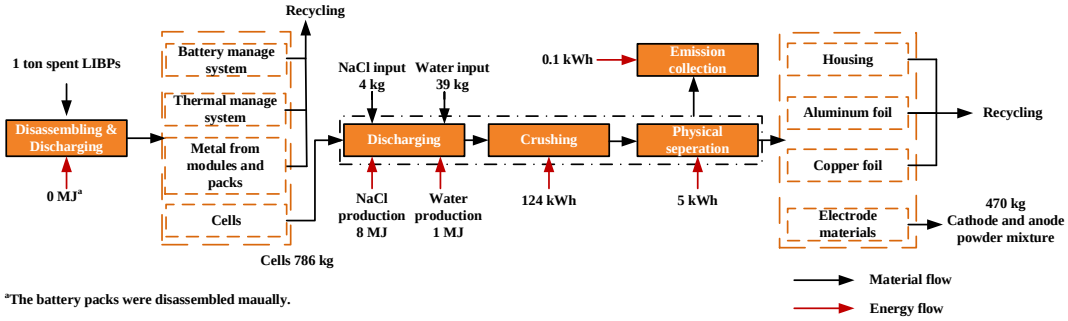

Figure S2. Energy and material flows in the pretreatment phase of spent LIB recycling system.

LIBPs from different manufacturers usually has different structural design. Therefore, it is of great challenge to achieve the automatic disassembly of the LIBPs [29, 31-33]. To separate the components of the LIBPs and to enrich its valuable part for further processing, pretreatment is an inevitable procedure as presented in Fig. S2. We assumed that the discharging and disassembling of LIBPs were completed manually at this stage, and thus the energy consumption of this step was 0 MJ.

The 786 kg LIB cells obtained from the discharging and disassembling step were further processed, and the main components such as battery management system (BMS), thermal management system (TMS), and housings of packs and modules were recovered as shown in Fig. S2. Then, further discharging of these cells was completed by immersing in 10 wt% NaCl solution [34] to ensure the safety during crushing[32, 35]. In the step, we assumed that the mass ratio of the immersion solution to the cells was 2:1, and the reuse rate of brine was 90% according to our

experiments. The NaCl and water consumption during the treatment of these LIBs was 4 and 39 kg, corresponding to a production energy consumption of 8 and 1 MJ for NaCl and water, respectively.

After discharging, the cells were mechanically crushed to facilitate the subsequent physical separation and pyrometallurgical or hydrometallurgical conversion. According to ref. [3], the energy consumption for crushing 786 kg cells was 124 kWh (158 kWh t^{-1} LIBs). After crushing, a physical separation of the components was conducted with an energy consumption of 5 kWh (6 kWh t^{-1} LIBs [3]). Then, the 470 kg electrode material mixture was obtained for further processing. At the same time, the main components of the cells such as cell housings, Cu and Al current collectors were recovered. To avoid the toxic gas emissions, the pretreatment steps were carried out in a semi-closed system with three centrifugal fans (DPT15-50A, 380 m^3 h^{-1},40 W) according to the minimum ventilation volume of 235.16 m^3 h^{-1} for processing 1 ton of LIBs [34]. Therefore, the energy consumption for ventilation and emission collection was 0.1 kWh.

3. Conversion phase

Since the processing method of regeneration phase is directly related to conversion phase, these two phases were analyzed together for each method.

3.1 UHT method

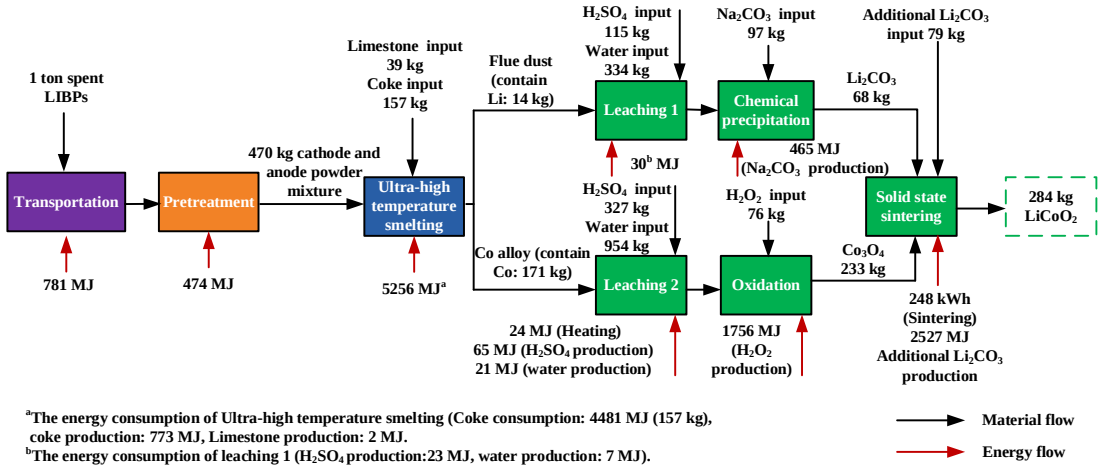

Figure S3. Flow diagram of the UHT method.

The material and energy consumption calculations of the UHT smelting step were based on the smelting step of the Umicore process [3, 36]. The energy and material flows for the process were displayed in Fig. S3. According to ref. [3, 36], the treatment of 470 kg powder mixture needs 157 and 39 kg of coke and limestone, corresponding to an energy consumption of 4481 MJ from coke burning and 775 MJ for material productions, respectively. Therefore, the total energy consumption for the UHT smelting step was 5256 MJ. And then the obtained cobalt alloy (containing 171 kg Co at a Co recovery rate of 98% [36]) and lithium-rich flue dust (containing 14 kg Li at a recovery rate of 68.6%[37]) were treated by leaching processes. In detail, we assumed that the leaching and chemical precipitation of Li consumed a negligible amount of energy but included the burden of H_2SO_4, Na_2CO_3 and water production for these steps. The reagent consumptions were calculated at 1.15 times of theoretical stoichiometric requirement for 3.5 M H_2SO_4 [38, 39] and a theoretical

stoichiometric level of Na_2CO_3. Thus, the corresponding material consumption for Li extraction from 70 kg Li-rich flue dust [37] were 115 kg for H_2SO_4, 334 kg for water, and 97 kg for Na_2CO_3, yielding 68 kg Li_2CO_3 by assuming a leaching rate of 90% [37]. The estimation of Co alloy leaching was similar to Li leaching excepted that a very little energy (0.13 MJ kg^{-1}) was required for heating provided by a 90% efficiency electric heater based on the average value of two similar industrial processes [3, 40]. The sequential oxidation step was assumed to operate at room temperature and thus no energy was needed. While, a theoretical stoichiometric ratio of H_2O_2 was assumed to be adopted as an oxidizer according to ref. [3]. Finally, the estimation of Li_2CO_3 consumption was based on a theoretical stoichiometric ratio to enable the Co_3O_4 complete reusing at sintering step. Thus, the recovered 68 kg Li_2CO_3 and 233 kg Co_3O_4 plus 79 kg of additional virgin Li_2CO_3 were sintered together in an electric furnace (98% electricity efficiency) to produce 284 kg LCO. The power consumption of the sintering process was calculated based on the values (2.11 MJ kg^{-1} fed materials, assumed a 90% efficiency of electric furnace) provided in ref. [3], corresponding to an energy consumption of 248 kWh.

3.2 Hydrometallurgical method

A well-reported strong acid (sulfuric acid) and organic acid (citric acid) were adopted in this study. The design of the industrial-scaled processes of the HM-SA and HM-CA methods shown in Figs. S4 and S5 was based on refs. [11, 15, 21, 24, 26, 41-45]. During these processes, 470 kg powder mixture of anode and cathode materials (cathode: 290 kg, anode: 180 kg) obtained from the pretreatment phase was leached by H_2SO_4 or citric acid, then filtered, chemically precipitated, and solid-state sintered to generate LCO.

3.2.1 HM-SA method

The reagent consumptions during sulfuric acid leaching were calculated based on the average laboratory data reported in literatures [21-28], shown in Table S6. To achieve an acceptable leaching efficiency, 2 times of stoichiometric requirement of 2M H_2SO_4 and 6 times of stoichiometric requirement of H_2O_2 were used in this study according to Eq. (1) and Table S6.

$$2LiCoO_2\,(s) + H_2O_2\,(aq) + 3H_2SO_4\,(aq) = 2Co^{2+}\,(aq) + O_2\,(g) + 2Li^{+}\,(aq) + 4H_2O + 3SO_4{}^{2-}\,(aq) \quad (1)$$

Similar to cobalt alloy leaching in Section 3.1, the energy consumption in heating during leaching step was used according to two similar industrial processes. The energy consumption of filtration step was 0.32 MJ kg^{-1} solids according to ref. [3]. In the precipitation step, Na_2CO_3 was used as the precipitator and was provided at a theoretical stoichiometric level [43-45]. Finally, similar to the UHT method in Section 3.1, 104 kg of Li_2CO_3 and 335 kg of $CoCO_3$ yielded from chemical precipitation (95% of the metals was assumed to be recovered), were sintered together [43-45], regenerating 276 kg of LCO.

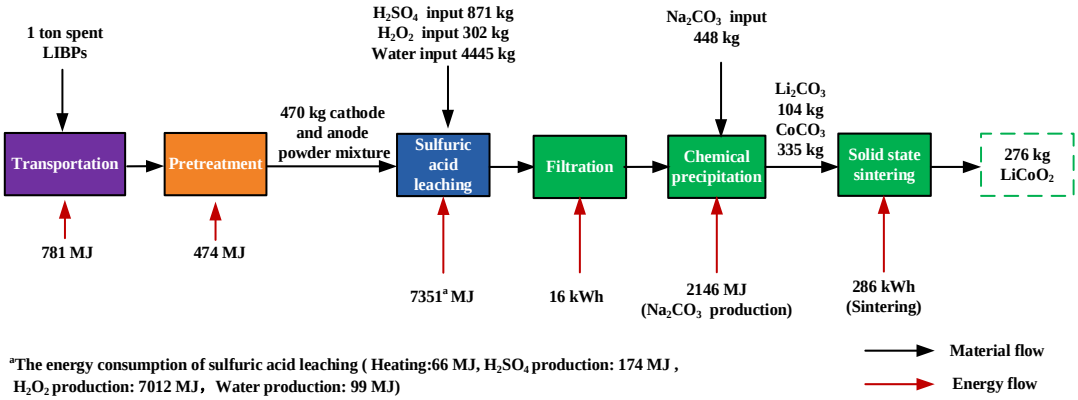

Figure S4. Flow diagram of the HM-SA method.

3.2.2 HM-CA method

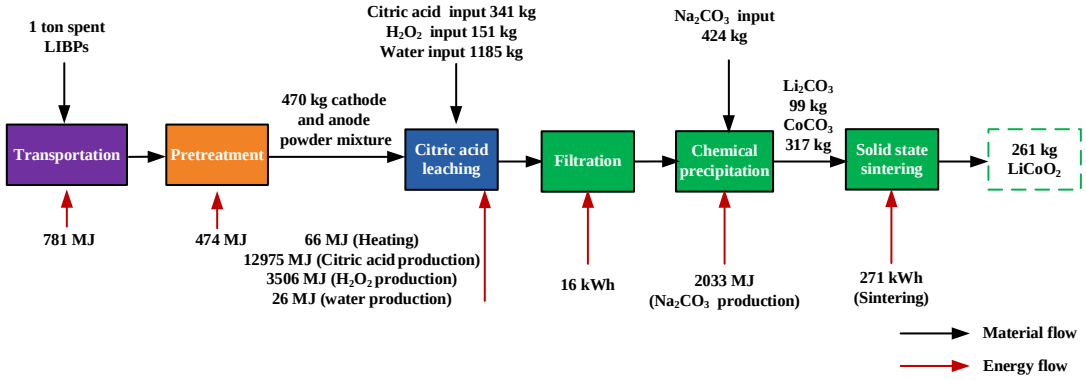

Figure S5. Flow diagram of the HM-CA method.

The energy and material flows of this method were detailed in Fig. S5. During the organic acid leaching process, citric acid was used as the leachant due to the advantages of less expensive, high leaching efficiency, and lower production energy consumption compared to other organic acids [21, 24, 26, 40]. The reagent consumptions of citric acid leaching were also calculated based on the average laboratory data reported in literatures [21-28], shown in Table S7, which were 6 times theoretical stoichiometric ratio of 1.5M citric acid and 4 times theoretical stoichiometric level of H_2O_2. And 90% of the metals was assumed to be recovered. In addition, 90% of the used citric acid was assumed to be recovered and reused based on ref. [3, 21, 42], and the recovery of waste acid and related treatments were not included in our calculation. The reaction equations are as followed:

$$6H_3Cit(aq) + 2LiCoO_2(s) + H_2O_2(aq) = 2Li^+(aq) + 2Co^{2+}(aq) + 6H_2Cit^-(aq) + 4H_2O + O_2(g) \quad (2)$$

$$6H_2Cit^-(aq) + 2LiCoO_2(s) + H_2O_2(aq) = 2Li^+(aq) + 2Co^{2+}(aq) + 6HCit^{2-}(aq) + 4H_2O + O_2(g) \quad (3)$$

$$6HCit^{2-}(aq) + 2LiCoO_2(s) + H_2O_2(aq) = 2Li^+(aq) + 2Co^{2+}(aq) + 6Cit^{3-}(aq) +$$

$$4H_2O + O_2(g) \quad (4)$$

3.3 In-situ RR Method

In this study, the graphite in LIB anode is used directly as a reductant and the life-cycle impact was quantified by estimating roasting the anode and cathode material under N_2 atmosphere (RR-N_2) and vaccine conditions (RR-vac). Based on refs. [38, 39, 46-50], the industrial-scaled technical processes for RR-N_2 and RR-vac were designed as shown in Figs. S6 and S7, respectively.

3.3.1 RR-N_2 method

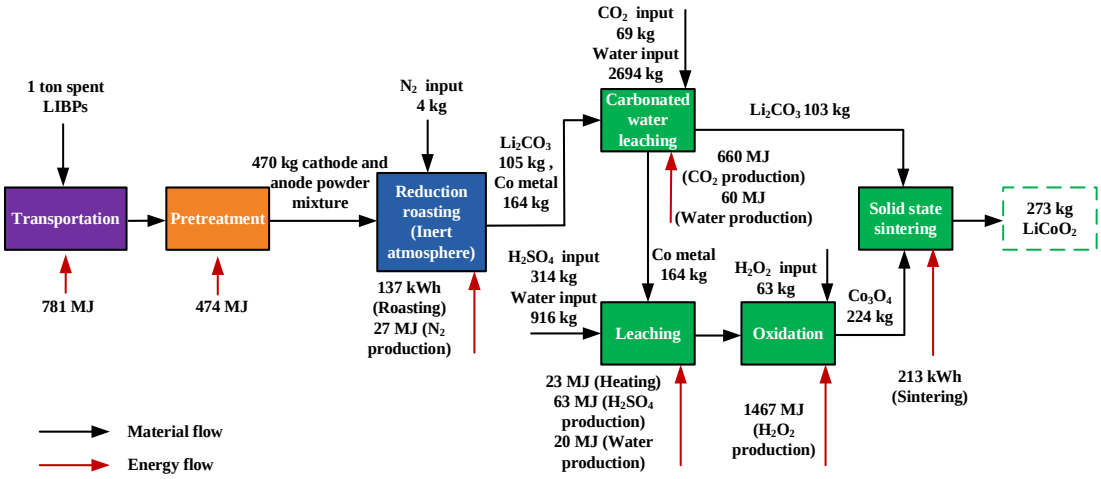

Figure S6. Flow diagram of the RR-N_2 method.

In RR-N_2 process, 470 kg of electrode powder mixture obtained from pretreatment was first in-situ roasted for 30 min at 850°C in a N_2 atmosphere [51]. To estimate the energy consumption during roasting, we assumed that the volume of the chamber furnace was 8300 L with a 33% volume utilization rate and the roasting temperature is 850 °C operating at a full power of 200 kW. It is estimated that the amount of electrode powder mixture treated in single batch was 4109 kg base on the assumption that the density of powder mixture was calculated by 1.5 kg L^{-1}[52]. The N_2 consumption was estimated to be 30096 L per batch based on a similar industrial process in ref. [53]. Therefore, the energy consumption during RR-N_2 process can be calculated using the following equations:

$$Q_{total} = Q_{oven} + Q_{reactants} \quad (5)$$

$$Q_{oven} = \frac{P_0 \times t_0}{3.6} \quad (6)$$

$$Q_{reactants} = \frac{m \times C_p \times \Delta T}{1000 \times \eta} \quad (7)$$

Where Q_{total} is the total energy consumption during RR-N_2 process (MJ), Q_{oven} is the energy consumption for furnace heating(MJ), P_o is the heating power(kW), t_o is the heating time(h), $Q_{reactants}$ is the energy consumption for heating the mixture of electrode materials(MJ), m is the total mass of mixture of electrode materials(kg), C_p represents the heat capacity of the mixture of electrode material (1.05 kJ kg^{-1} K^{-1} [52]), ΔT is the temperature difference(K), and η is the efficiency of electric furnace (90%).

It is estimated that when the 470 kg of powder mixture was treated in RR-N_2 process, 4 kg FU^{-1} of N_2 was consumed, yielding 164 kg of cobalt and 105 kg of Li_2CO_3 based on the assumption that the recovery rate of cobalt and lithium was 94.12% and 95.98%, respectively [51]). The energy consumptions of the furnace and N_2 production were 137 kWh and 27 MJ, respectively. Then, the recovered cobalt and Li_2CO_3 were separated by carbonated water leaching at a liquid-solid ratio of 10 ml g^{-1} [39] and 1.1 times of theoretical stoichiometric amount of CO_2 according to the following reaction:

$$Li_2CO_3\,(s) + H_2O\,(aq) + CO_2(g) = 2LiHCO_3(aq) \quad (8)$$

This step consumed 69 kg CO_2 and 2694 kg water, and the production energy consumption was 660 and 60 MJ for CO_2 and water, respectively. The recovered 164 kg cobalt metal was leached and oxidized to obtain 224 kg Co_3O_4. Finally, the recovered 103 kg Li_2CO_3 and 224 kg Co_3O_4 were solid-state sintered, yielding 273 kg LCO.

3.3.2 RR-Vac method

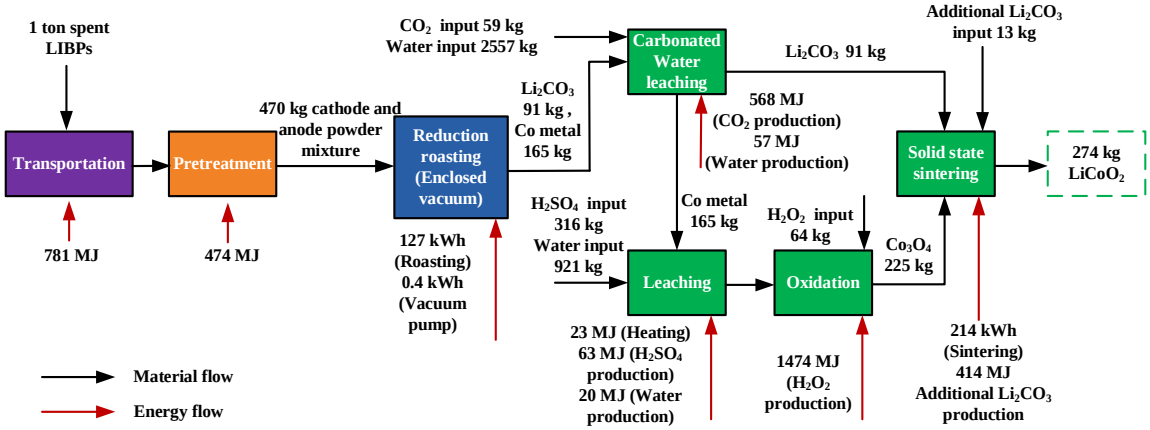

Figure S7. Flow diagram of the RR-Vac method.

The energy and material flows of RR-Vac were detailed in Fig. S7. The life-cycle impact estimation of RR-Vac was carried out in a similar way as RR-N_2 except that the powder mixture was roasted at 800°C in a vacuum condition [47, 48]. During the RR-vac process, a vacuum pump was used to evacuate the chamber furnace to 1000 Pa, and then the vacuum pump was shut off, while a furnace with a heat power of 100 kW was sealed and heated for 45 min. Based on the method in the design manual [54], a unit of two-stage Roots oil ring pump was selected to estimate the energy consumption during the vacuum-pumping process. The time (t_p) required for vacuum-pumping was estimated to be 0.35 h according to Eq. 9.

$$t_p = 2.3 \times \left(\frac{V}{S}\right) \times \log\left(\frac{P_i}{P}\right) \quad (9)$$

Where V is the volume of the furnace (8300L), S is the pumping rate of the vacuum pump (30 L s^{-1}), P_i is the atmospheric pressure (101.325 kPa), and P is the target pressure in the furnace (1 kPa). Therefore, the energy consumption for vacuum pumping (W_p) can be calculated according to Eq. 10.

$$W_p = t_p \times (\frac{P_1}{\eta_1} + \frac{P_2}{\eta_2}) \quad (10)$$

Where P_1 is the power of the first-stage pump (4.75 kW), η_1 is the efficiency of the first-stage pump (80%), P_2 is the power of the second-stage pump (2.95 kW), and η_2 is the efficiency of the second-stage pump (70%)[54]. The energy consumption of vacuum pumping for a single batch was 3.6 kWh, which was equivalent to 0.4 kWh FU^{-1}. Similar to section 3.3.1, to process 470 kg powder mixture, the energy consumption of the furnace was 127 kWh, yielding 165 kg cobalt metal and 91 kg Li_2CO_3 based on the assumption that the recovery rates of cobalt and lithium were 94.59% [49] and 82.7% [48], respectively). Then, the roasted products were treated in the same way as RR-N_2, producing 274 kg LCO.

References:

1. Nelson, P.A.G., K. G.; Bloom, I.; Dees, D. W., *Modeling the Performance and Cost of Lithium-Ion Batteries for Electric-Drive Vehicles*. 2011, Argonne National Lab. (ANL), Argonne, IL: United States.
2. Dunn, J.B., et al., *Material and Energy Flows in the Production of Cathode and Anode Materials for Lithium Ion Batteries*. 2015, Argonne National Lab. (ANL): United States.
3. Dunn, J.B., Gaines, L, Barnes, M, Wang, M, and Sullivan, J., *Material and Energy Flows in the Materials Production, Assembly, and End-of-Life Stages of the Automotive Lithium-Ion Battery Life Cycle*. 2012, Argonne National Lab. (ANL): United States.
4. Ellingsen, L.A.-W., et al., *Life Cycle Assessment of a Lithium-Ion Battery Vehicle Pack.* Journal of Industrial Ecology, 2014. **18**(1): p. 113-124.
5. Diekmann, J., et al., *Ecological Recycling of Lithium-Ion Batteries from Electric Vehicles with Focus on Mechanical Processes.* Journal of The Electrochemical Society, 2016. **164**(1): p. A6184-A6191.
6. Ciez, R.E. and J.F. Whitacre, *Examining different recycling processes for lithium-ion batteries.* Nature Sustainability, 2019. **2**(2): p. 148-156.
7. Ning, D., et al., *Comparative analysis of primary aluminum and recycled aluminum on energy consumption and greenhouse gas emission.* The Chinese Journal of Nonferrous Metals, 2012. **22**(10).
8. Dunn, J.B., et al., *Impact of recycling on cradle-to-gate energy consumption and greenhouse gas emissions of automotive lithium-ion batteries.* Environmental Science & Technology, 2012. **46**(22): p. 12704-10.
9. Dunn, J.B., et al., *The significance of Li-ion batteries in electric vehicle life-cycle energy and emissions and recycling's role in its reduction.* Energy & Environmental Science, 2015. **8**(1): p. 158-168.
10. Xie, J.-b., et al., *Evaluation of mixed heat effect of fuel gas and coke in steelmaking flue.* Journal of Thermal Analysis and Calorimetry, 2018. **137**(1): p. 245-252.
11. Shin, S.M., et al., *Development of a metal recovery process from Li-ion battery wastes.* Hydrometallurgy, 2005. **79**(3-4): p. 172-181.
12. Swain, B., et al., *Hydrometallurgical process for recovery of cobalt from waste cathodic active material generated during manufacturing of lithium ion batteries.* Journal of Power Sources, 2007. **167**(2): p. 536-544.
13. Dorella, G. and M.B. Mansur, *A study of the separation of cobalt from spent Li-ion battery*

residues. Journal of Power Sources, 2007. **170**(1): p. 210-215.
14. Ferreira, D.A., et al., *Hydrometallurgical separation of aluminium, cobalt, copper and lithium from spent Li-ion batteries.* Journal of Power Sources, 2009. **187**(1): p. 238-246.
15. Kang, J., et al., *Recovery of cobalt sulfate from spent lithium ion batteries by reductive leaching and solvent extraction with Cyanex 272.* Hydrometallurgy, 2010. **100**(3-4): p. 168-171.
16. Sun, L. and K. Qiu, *Vacuum pyrolysis and hydrometallurgical process for the recovery of valuable metals from spent lithium-ion batteries.* J Hazard Mater, 2011. **194**: p. 378-84.
17. Chen, L., et al., *Process for the recovery of cobalt oxalate from spent lithium-ion batteries.* Hydrometallurgy, 2011. **108**(1-2): p. 80-86.
18. Zhu, S.-g., et al., *Recovery of Co and Li from spent lithium-ion batteries by combination method of acid leaching and chemical precipitation.* Transactions of Nonferrous Metals Society of China, 2012. **22**(9): p. 2274-2281.
19. Jha, M.K., et al., *Recovery of lithium and cobalt from waste lithium ion batteries of mobile phone.* Waste Management, 2013. **33**(9): p. 1890-7.
20. Bertuol, D.A., et al., *Recovery of cobalt from spent lithium-ion batteries using supercritical carbon dioxide extraction.* Waste Manag, 2016. **51**: p. 245-251.
21. Chen, X., et al., *Sustainable Recovery of Metals from Spent Lithium-Ion Batteries: A Green Process.* ACS Sustainable Chemistry & Engineering, 2015. **3**(12): p. 3104-3113.
22. Li, L., et al., *Recovery of cobalt and lithium from spent lithium ion batteries using organic citric acid as leachant.* J Hazard Mater, 2010. **176**(1-3): p. 288-93.
23. Golmohammadzadeh, R., F. Rashchi, and E. Vahidi, *Recovery of lithium and cobalt from spent lithium-ion batteries using organic acids: Process optimization and kinetic aspects.* Waste Manag, 2017. **64**: p. 244-254.
24. Yu, M., et al., *A more simple and efficient process for recovery of cobalt and lithium from spent lithium-ion batteries with citric acid.* Separation and Purification Technology, 2019. **215**: p. 398-402.
25. Santana, I.L., et al., *Photocatalytic properties of Co3O4/LiCoO2 recycled from spent lithium-ion batteries using citric acid as leaching agent.* Materials Chemistry and Physics, 2017. **190**: p. 38-44.
26. Almeida, J.R., et al., *Composition analysis of the cathode active material of spent Li-ion batteries leached in citric acid solution: A study to monitor and assist recycling processes.* Sci Total Environ, 2019. **685**: p. 589-595.
27. Dos Santos, C.S., et al., *A closed-loop process to recover Li and Co compounds and to resynthesize LiCoO2 from spent mobile phone batteries.* J Hazard Mater, 2019. **362**: p. 458-466.
28. Li, L., et al., *Recovery of valuable metals from spent lithium-ion batteries by ultrasonic-assisted leaching process.* Journal of Power Sources, 2014. **262**: p. 380-385.
29. Chen, M., et al., *Recycling End-of-Life Electric Vehicle Lithium-Ion Batteries.* Joule, 2019. **3**(11): p. 2622-2646.
30. Wang, Q., et al., *A review of lithium ion battery failure mechanisms and fire prevention strategies.* Progress in Energy and Combustion Science, 2019. **73**: p. 95-131.
31. Herrmann, C., et al. *Assessment of Automation Potentials for the Disassembly of Automotive Lithium Ion Battery Systems*. 2012. Berlin, Heidelberg: Springer Berlin Heidelberg.

32. Kwade, A. and J. Diekmann, *Recycling of Lithium-Ion Batteries*. 1 ed. Sustainable Production, Life Cycle Engineering and Management, ed. C. Herrmann and S. Kara. 2018: Springer International Publishing.
33. Harper, G., et al., *Recycling lithium-ion batteries from electric vehicles.* Nature, 2019. **575**(7781): p. 75-86.
34. Li, J., G. Wang, and Z. Xu, *Generation and detection of metal ions and volatile organic compounds (VOCs) emissions from the pretreatment processes for recycling spent lithium-ion batteries.* Waste Management, 2016. **52**: p. 221-227.
35. Sonoc, A., J. Jeswiet, and V.K. Soo, *Opportunities to Improve Recycling of Automotive Lithium Ion Batteries.* Procedia CIRP, 2015. **29**: p. 752-757.
36. Daniel Cheret, S.B.S.S., Hofors (SE). *Battery Recycling*. 2007: United States
37. Georgi-Maschler, T., et al., *Development of a recycling process for Li-ion batteries.* Journal of Power Sources, 2012. **207**: p. 173-182.
38. Hu, J., et al., *A promising approach for the recovery of high value-added metals from spent lithium-ion batteries.* Journal of Power Sources, 2017. **351**: p. 192-199.
39. Zhang, J., et al., *Efficient and economical recovery of lithium, cobalt, nickel, manganese from cathode scrap of spent lithium-ion batteries.* Journal of Cleaner Production, 2018. **204**: p. 437-446.
40. Li, L., et al., *Recovery of metals from spent lithium-ion batteries with organic acids as leaching reagents and environmental assessment.* Journal of Power Sources, 2013. **233**: p. 180-189.
41. Xu, J., et al., *A review of processes and technologies for the recycling of lithium-ion secondary batteries.* Journal of Power Sources, 2008. **177**(2): p. 512-527.
42. Chen, X., et al., *An atom-economic process for the recovery of high value-added metals from spent lithium-ion batteries.* Journal of Cleaner Production, 2016. **112**: p. 3562-3570.
43. Yang, H., et al., *Research on Structure and Properties of LiCoO2 Prepared from Spent Lithium Ion Batteries.* Rare Metal Materials and Engineering, 2006. **35**(5): p. 836-840.
44. Granata, G., et al., *Product recovery from Li-ion battery wastes coming from an industrial pre-treatment plant: Lab scale tests and process simulations.* Journal of Power Sources, 2012. **206**: p. 393-401.
45. Wang, B., et al., *Recycling LiCoO2 with methanesulfonic acid for regeneration of lithium-ion battery electrode materials.* Journal of Power Sources, 2019. **436**: p. 226828 (1-9).
46. Li, J., G. Wang, and Z. Xu, *Environmentally-friendly oxygen-free roasting/wet magnetic separation technology for in situ recycling cobalt, lithium carbonate and graphite from spent LiCoO2/graphite lithium batteries.* Journal of Hazardous Materials, 2016. **302**: p. 97-104.
47. Xiao, J., J. Li, and Z. Xu, *Recycling metals from lithium ion battery by mechanical separation and vacuum metallurgy.* Journal of Hazardous Materials, 2017. **338**: p. 124-131.
48. Xiao, J., J. Li, and Z. Xu, *Novel Approach for in Situ Recovery of Lithium Carbonate from Spent Lithium Ion Batteries Using Vacuum Metallurgy.* Environ Sci Technol, 2017. **51**(20): p. 11960-11966.
49. Huang, Z., et al., *Characterization of the Materials in Waste Power Banks and the Green Recovery Process.* ACS Sustainable Chemistry & Engineering, 2018. **6**(3): p. 3815-3822.
50. Mao, J., J. Li, and Z. Xu, *Coupling reactions and collapsing model in the roasting process of recycling metals from LiCoO2 batteries.* Journal of Cleaner Production, 2018. **205**: p. 923-929.
51. Li, J., G. Wang, and Z. Xu, *Environmentally-friendly oxygen-free roasting/wet magnetic*

separation technology for in situ recycling cobalt, lithium carbonate and graphite from spent LiCoO2/graphite lithium batteries. J Hazard Mater, 2016. **302**: p. 97-104.

52. Dunn, J.B., et al., *Material and Energy Flows in the Production of Cathode and Anode Materials for Lithium Ion Batteries.* Acta Chemica Scandinavica, 2015. **49**(24): p. 44-52.
53. Luo, X., et al., *Design and Application of Mesh Belt Furnace for LiFeO4.* Industrial Heating, 2009. **38**(02): p. 47-49.
54. Da, D., *Vacuum design manual*. 3rd ed. 2004: National defense industry press.